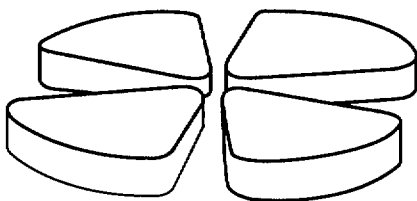




FR9800314

GANIL



Gestion INIS
Doc. enreg. le : 11/3/98
N° TRN :
Destination : I.R.S.D

Neutron and Energy Production by Energetic Projectiles: Protons or Deuterons?

D. Ridikas and W. Mittig

GANIL, BP 5027, F-14076 CAEN Cedex 5, France

GANIL P 98 02

29-43

R

Neutron and Energy Production by Energetic Projectiles: Protons or Deuterons?

D. Ridikas and W. Mittig

GANIL, BP 5027, F-14076 CAEN Cedex 5, France

February 12, 1998

Abstract

A revival of interest for production of neutrons by light energetic projectiles has been arisen recently by the advent of new projects in nuclear technology such as accelerator driven nuclear reactors, nuclear waste transmutation and the use of radioactive beams. In this context we try to estimate which of the light incident particles, namely protons or deuterons, are more favourable for neutron production. The problem is investigated by varying the incident energy of these projectiles for different target materials and assemblies. The averaged multiplicities, angular and energy distributions of neutrons produced are presented and compared using the simplest target geometry. In addition, the energy gain factor, i.e. the ratio of the energy produced in the sub-critical target-reactor to the one delivered by the beam, is estimated for both of the incident particles as a function of their kinetic energy. It is shown that at lower energies ($\leq 600\text{MeV}$), the combination of deuteron beam with light target is the most efficient solution for energy generation, whereas at higher energies ($\geq 1\text{GeV}$) the difference between various combinations becomes less significant.

1 Introduction

The use of neutrons for transmutation of the long-lived radioactive nuclei of nuclear waste to stable or short-lived species has been under consideration already for many years [1]. When an energetic particle hits the target material consisting of heavy nuclei, tens of neutrons might be generated. This is of course, the feature of outermost importance for the so-called subcritical hybrid systems (see [2, 3, 4] and Refs. therein). The interest in neutron production reactions has been recently renewed because they are the basis in the development of powerful neutron sources for various purposes like nuclear energy production and incineration of nuclear waste, material structure analysis, tritium production, etc. Another interest is related to the possibility of the production of radioactive nuclei and exotic beams by neutron induced fission [5, 6]. One of the crucial problems in this context is to determine the most efficient way to convert the beam energy into neutrons produced afterwards.

So far only high energy (0.8 – 1.6 GeV) protons hitting a heavy target (uranium, thorium, lead) were considered as far as subcritical hybrid systems are concerned [2, 3, 4]. The use of projectiles such as deuterons and light targets as converters to create the neutrons may have competitive, if not more efficient, features too. This possibility was noticed by E.O. Lawrence already in 1947 after the very first experiments at the newly installed 184 inches cyclotron at Berkeley. Amusingly enough, it was also very early recognized that spallation reactions could be used for producing ^{239}Pu from depleted uranium and as an external source for neutrons for fission reactors (already almost the concept of the energy amplifier!) [7].

ABS In this report we ~~present and compare~~ *are presented and compared.* The predictions of neutron production induced by deuterons and protons with the LAHET code system [8]. ~~We consider~~ *are considered* the incident energy of the projectiles, averaged neutron multiplicities, angular and energy distributions of emitted neutrons from different target materials and their further multiplication in the multiplying medium as the most important parameters of our interest. The energy gain in the simplified sub-critical target assembly is estimated and compared for both of the incident particles as a function of their kinetic energy.

2 The LAHET code system (LCS)

Many theories have been formulated to describe preequilibrium phenomena induced by various projectiles. Among them are the intranuclear cascade model [9], the quasi-free scattering model [10], the preequilibrium exciton model [11, 12],

and hybrid model [13]. These various models have been reasonably successful in accounting for a large body of experimental data. The LAHET code [8] employs the most popular theoretical approach to spallation reactions, namely the intranuclear cascade (INC) and evaporation models. As an alternative to the Bertini INC [14], this code contains the INC routines from the ISABEL code. The ISABEL INC model is an extension by Yariv and Fraenkel [15] of the VEGAS code [16]. It has the capability of treating nucleus-nucleus interactions as well as particle-nucleus interactions.

LAHET includes two models of fission induced by high energy interactions: the ORNL model by Alsmiller et al. [18] and the RAL model by Atchison [19]. The fission models are employed with the evaporation model of Dresner [20]. The Fermi breakup model [21] has replaced the evaporation model for the disintegration of light nuclei ($A \leq 17$). In the LAHET implementation, only two- and three-body breakup channels are considered.

LAHET also contains the multistage preequilibrium exciton model (MPM) as described in [22]. The MPM is invoked at the completion of the INC, and at each stage in the MPM, the excited nucleus may emit a neutron, proton, deuteron, triton, ^3He or alpha. The MPM terminates upon reaching the equilibrium exciton numbers; the evaporation model (or the Fermi breakup model for light nuclei) is applied to the residual nucleus with the remaining excitation energy.

LAHET differs from the HETC code [20] in the use of cutoff energies of particles escaping from the nucleus during the INC. The default procedure is to apply a fixed cutoff barrier for neutrons equal to the mean binding energy of one proton and one neutron with respect to the target nucleus; escaping particles with final energy below the cutoff are retained by the nucleus. For protons, the cutoff energy is the maximum of the neutron cutoff energy and a Coulomb barrier.

LAHET may also be used to compute cross sections directly. With this option, the transport is turned off and the primary particle is assumed to interact directly with the specified material at the incident energy. The history file produced is then processed with XSEX code to generate double-differential particle production cross sections.

For ejectile energies $E \leq 20$ MeV the neutron transport is performed using the MCNP code [23] utilizing ENDF/B-based neutron cross section libraries. LAHET employs the same geometry system as MCNP. Both of these code systems and subsequent post-processing codes are installed at GANIL [24, 25].

We have examined the LCS system with existing neutron production cross section and multiplicity measurements (see, for example, 50MeV Be(d,xn) [26], 190MeV Be, U(d,xn) [7], 188MeV Pb(d,xn) and 197MeV Pb(p,xn) [27], 475MeV Au,U(p,xn) [28], 540MeV Be, Pb, U(p,xn) [29]). A characteristic narrow peak

at large energies for emitted neutrons (almost the incident energy), which is well seen at forward angles, and which fades out with increasing scattering angle, is not properly reproduced for direct deuteron breakup on heavy targets (see [29] for experimental data and more detailed discussion). Following our estimations, we found that the missing part of this process contributes less than 2% to the total neutron production cross section, and it becomes less important for lighter targets. For measured neutron multiplicities we obtained a reasonable agreement (within 10-15%) comparing to the values predicted by the LCS. In addition, we refer the reader to Ref. [8], where the results from running LAHET and subsequent post-processing codes have been compared extensively against experimental data in a multitude of varying target materials, projectile particle type and energy, and geometry. However, there is no much new and systematic data available on neutron multiplicity measurements within the energy region of $50 \text{ MeV} \leq E_{proj.} \leq 600 \text{ MeV}$, in particular for reactions induced by deuterons. Therefore, both (p,xn) and (d,xn) experiments at these energies are strongly desired.

We have to note at this point, that the neutron multiplicities recently reported by J. Cugnon *et al.* [30] cannot be directly compared to our calculated values. The authors in this paper performed the calculations for infinitely thin targets without any particle transport in materials. That means only elementary interactions through intranuclear cascades and evaporations are taken into account, and the final neutron multiplicities do not depend on the target geometry [31], what is not true in the case of our calculations.

3 Total neutron yield

From the very beginning, a deuteron already carrying one neutron, seems to be more efficient for neutron production than a proton. Consequently, an α particle, with two neutrons and two protons, would be more favourable in the same context. As a matter of fact, the situation is more complicated. In Figure 1 we present calculated averaged neutron multiplicities normalized per incident particle for protons, deuterons and α particles at the incident energy of 100MeV/nucleon on different target materials. When the nucleus is bombarded with 200MeV deuterons, or 400MeV α particles, the binding energy of the incident nucleons is important chiefly in causing a spatial correlation between them, and what happens can be thought of in terms of a simultaneous bombardment by several individual nucleons. Their characteristics depend primarily on the fact that the deuteron is a very loosely bound system with the proton and neutron

actually spending most of their time outside the range of their mutual forces. Contrary, α particle is more bound by one order of magnitude if compared to deuteron. It is also clear that neutron production by protons in this picture is very low as long as all incident particles have the same energy per nucleon. The target dependence of the neutron yield (here we refer to the shapes of the curves) is quite similar for all projectiles: the neutron production is more favourable for very light (lithium or beryllium) and very heavy (thorium or uranium) target materials.

Since the total energy is one of the essential parameters which defines the actual costs of particle acceleration, it is more reasonable to compare neutron production by protons and deuterons at the same total incident energies. Figure 2 represents total neutron yield from proton (p) and deuteron (d) induced reactions as a function of three incident energies and a number of target materials. The target thicknesses in (cm) are given in Table 1 explicitly for some of the materials and incident energies. For all energies deuterons are much more efficient in neutron production if one chooses very light targets. In the case of Be, neutron yield is higher for deuterons by a factor of 1.5-2.5 depending on energy, and the difference decreases with increase in incident energy. Nevertheless, even at 1GeV deuterons are more efficient by a factor of 1.3 (see Figure 3 for more qualitative comparison). However, that is not the case for heavy targets. Here at 200MeV neutron production by protons and deuterons is almost the same. Increase in projectile energy makes deuterons more efficient only by 10% for U, for example, if compared to protons. Contrary, neutron multiplicities at 80MeV protons and deuterons are higher for protons. We found that at these energies almost no secondary neutrons (neutrons produced by other particles than incident particles, by (n,xn) process, for example) are produced, and primary neutron production by protons is more efficient. It is also very important to notice that neutron yield from light targets is comparable to the one from heavy targets only by deuteron induced reactions, while protons always produce considerably more neutrons on heavy targets than on the light ones (see Figure 2).

4 Angular and energy distributions of neutrons

If we compare the angular distribution curves for neutron production by protons and deuterons at 200MeV in Figure 4, there is one feature in common: in the case of protons, the angular distributions are relatively flat (upper part), while for deuteron induced reactions the neutron production is more concentrated at forward angles (lower part). On the other hand, both (p,xn) and (d,xn) reactions

show a somewhat similar angular dependence at more backward angles; the cross section decreases considerably with the angle in the case of Be and Fe, while for the U target neutrons are emitted in the entire scattering angle range. Here multiple nucleon scattering and secondary neutron production during the evaporation stage contribute mostly.

This observed difference might be very important in further investigations on neutron production within subcritical hybrid systems, where the use of light or heavy targets, in our opinion, is still an open question. One could think of the combined system, for example, with a light target as a converter in order to create the neutrons (which as we have shown are mostly emitted at forward angles for light targets) and a heavy target (placed right after the light target) to increase the neutron flux further. In this context (d,xn) reaction is much more favourable for two well established reasons. First of all, neutron production in absolute value is higher for light targets if one uses deuterons as we have shown in Chapter 3. Secondly, the neutrons created by deuterons in a light target are more forward peaked if compared to proton induced reaction; so these neutrons might be used more efficiently for secondary neutron production in a heavy target in terms of higher production rates and simpler geometry assemblies.

There is one more thing which has to be mentioned in this connection; it is clearly seen from Figure 5, where the energy distributions of neutrons emitted from (d,xn) and (p,xn) at 200MeV are presented, that much more energetic neutrons (note the log-log scale in the Figure) are produced by light targets than by heavy ones. The reader may find useful the numbers explicitly given in Table 2. Most of the neutrons (80%) from U fall into the energy interval from 0 to 5MeV, while more than 55% of neutrons from Be are emitted with energies higher than 10MeV. Moreover, deuterons (comparing to protons) both in light target and heavy target materials produce two times more energetic neutrons in absolute value (look for example, the line with $E_n \geq 25$ or $E_n \geq 50$ in Table 2). On the other hand, at the neutron energies of $E_n \geq 100$, protons overcome deuterons. Here we have to recall that deuterons have the incident energy of 100MeV/nucleon while for protons this number is 200MeV/nucleon. In spite of a very small percentage of these "super" energetic neutrons produced (7% for protons and just 2% for deuterons in the case of Be target to be compared to the total yield), these numbers might be crucial from the point of view of radioprotection. Here deuterons, making less "super" energetic neutrons, are in a better position again.

5 Simplified target assembly for neutron multiplication and energy production

In a charged particle induced cascade one can distinguish two qualitative physical regimes: a) a spallation driven, high energy phase and b) a neutron driven, fission dominated regime. Neutrons from the first phase are acting as a “source” for the second phase, in which they gradually lose energy by collisions and are multiplied by fissions and (n,xn) reactions. Depending on the final aim, one must choose very carefully the target materials for both of these physical regimes. In this Chapter we would like to develop in more detail the idea initiated already in 1952 during the measurements of neutron yields by bombardment of target assemblies with proton and deuterons beams. At that time two significant conclusions were reached [32]:

1. “In direct bombardment of (30cm) targets of uranium the yield in terms of neutrons per incident beam particle was 25% to 30% greater for deuterons than for protons of the same energy.”

2. “In the case of deuteron bombardment, the insertion of a one-range thickness of lithium or beryllium (primary target) in front of the uranium block (secondary target) resulted in nearly the same neutron yield as bombarding uranium directly...”

Encouraged by these findings and motivated by those we pointed out in the previous Chapters, a simplified sub-critical target assembly for neutron multiplication and energy production by proton and deuteron induced reactions was taken as a test case (see Figure 6). It consists of a spallation target (beryllium or uranium) inside a fuel assembly. For simplicity a homogeneous water and uranium mixture was used as a fuel. The device is surrounded by a spherical water blanket, acting as a “reflector”. The geometry parameters of the system are given in Table 3. We note that our simplified “reactor” can serve as a good approximation (as long as its geometry and materials are concerned) of a sub-critical arrangement made of natural uranium rods (0.71% ^{235}U) and water moderator as described in [33], where a measured effective neutron multiplication coefficient $k=0.895\pm 0.010$ was reported. We performed the criticality calculations with MCNP Monte Carlo code [23] by simulating a point-like neutron source placed in the middle of our spallation target. We found that the presence of ^{235}U in a fuel assembly has to be increased from 0.71% up to 0.95% for our simplified device in order to have the same k value within experimental error bars. With this configuration we obtained $k=0.887$. By replacing the uranium spallation target with a beryllium bar we observed only a small increase in k value (of the order

of 1%).

Our numerical results running LAHET+MCNP code systems [8, 23] for such a sub-critical “reactor” are shown in Tables 4 and 5. In addition to the total neutron multiplicities $\langle M_n \rangle$ normalized per incident beam particle, we also calculated the number of fissions N_{fiss} which took place in the fuel assembly and so called G-factor or energy gain in our combined system, i.e. the ratio of the energy produced in the device to the energy delivered by the beam. After each successive fission in ^{238}U or ^{235}U approximately 181MeV energy becomes available according to their fission Q-values. Therefore, the energy gain $G(N_{fiss})$ can be estimated by a very simple relation

$$G(N_{fiss}) = \frac{181 N_{fiss}}{E_{beam}}, \quad (1)$$

where E_{beam} is given in (MeV). Since our spallation target is surrounded by a multiplying medium with its effective multiplication factor k , the total number of neutrons after multiplication is $\frac{\langle M_n \rangle}{1-k}$; and the number of secondary neutrons is given by $\frac{k\langle M_n \rangle}{1-k}$. Performing the calculations we found that most of the secondary neutrons are produced by fission, which itself produces in average $\nu=2.47$ neutrons, while the contribution of secondary neutrons from the (n,xn) reaction was quite small. Therefore, an approximate expression relating the number of fissions N_{fiss} and neutron multiplicities $\langle M_n \rangle$ can be derived:

$$N_{fiss} = \frac{k \langle M_n \rangle}{\nu (1 - k)}. \quad (2)$$

Now from Eqs. 1 and 2 we can obtain another expression to calculate a G-factor, i.e.

$$G(\langle M_n \rangle) = \frac{181}{E_{beam}} \frac{k \langle M_n \rangle}{\nu (1 - k)}. \quad (3)$$

Both $G(N_{fiss})$ and $G(\langle M_n \rangle)$ values are given in Tables 4 and 5 for comparison. Note, that the $G(N_{fiss})$ as given by Eq. 1 should be more direct determination of the gain factor. A good agreement we obtained between the two ways to estimate this observable is somewhat “casual”. In other geometries, having the same criticality k , we observed much stronger discrepancies.

Table 4, which corresponds to the U+U target assembly, just confirms our results already discussed in Chapter 3; protons are almost equally efficient in neutron production at the same total incident energy if one chooses heavy metal target as lead, thorium or uranium. The difference depending on incident energy, chosen target material and its geometry, and ranges from 5% to 15% in favour of deuterons (see column $\langle M_n \rangle$ in Table 4 for uranium). Only a small difference was found for a number of fissions N_{fiss} in the multiplying material as well, what

results in nearly the same energy gain factor given by $G(\langle M_n \rangle)$ and $G(N_{fiss})$, i.e. only up to 10% higher for deuterons.

However, the Be+U target assembly (see Table 5) gives much higher neutron yields for deuterons as incident projectiles. In the case of deuterons, we obtained nearly the same neutron multiplicities as for U+U assembly, in agreement with the measurements back in 1952 [7]. In the case of protons, the $\langle M_n \rangle$ values are sharply decreased if compared to the ones obtained bombarding U spallation target directly (see $\langle M_n \rangle$ columns in Table 4 and Table 5 respectively). Moreover, the Be+U target combination with deuterons results in a faster increase of the number of fissions N_{fiss} (consequently in the energy gain factor $G(N_{fiss})$), as compared to the protons bombarding the U+U device (compare numbers in the columns $G(N_{fiss})$ of Table 4 for protons and Table 5 for deuterons)*. The reason for this difference is the following: as was already discussed above, neutrons originating from the light metal target are much more energetic; hence, their multiplication in the fissile material results in a higher number of fissions N_{fiss} (and energy gain $G(N_{fiss})$) per incident particle until the optimum incident energies are reached. Figure 7 shows the calculated energy gain $G(N_{fiss})$ as a function of the incident beam energy and two different spallation targets (Be or U) inside the same fuel assembly (uranium and water mixture) for protons and deuterons. In the same Figure we also plot the experimental points with error bars from [33], which in our notation should be compared to the “p on U+U” curve. In spite of the simplifications we made in our geometry assumptions, we got a reasonable agreement with the experimental data; the 5%-10% overestimation occurred most probably because in our calculations no neutron loss in the construction materials was taken into account. In addition, our predicted values for deuterons on Be+U target combination (see “d on Be+U” curve) suggest that a practical energy amplifier could therefore be operated with deuteron beam energies of the order of 400MeV-800MeV, i.e. at lower incident energies by 400MeV than suggested in [33] for proton beam, and still give a comparable energy gain factor.

There are more advantages of the light metal over heavy metal primary targets. In the case of light metal target + heavy metal target, the heat is distributed over a greater depth, and much of the beam power is carried forward into a secondary target by the high-energy neutrons. These neutrons penetrate the uranium assembly with much better efficiency having about a 10cm mean free path for interaction. So the fuel burnup should be more homogeneous if compared to the case when charged particles are stopped in the fuel assembly itself. If one

*It is important to note at this point, that at energies higher than 500MeV and 600MeV for protons and deuterons respectively, charged particles are not completely stopped in the Be bar, which is “allowed” to be only 80cm long because of the chosen size of the fuel assembly.

is interested in a high energy and forward peaked neutron source, for example for radioactive beam production or nuclear waste transmutation, again light metal targets are to be preferred together with deuterons as incident particles. Finally, if one plans to construct a test+demonstration sub-critical system of a high energy neutron source or an accelerator driven reactor, the separation of a target assembly into two in principle independent parts, namely the spallation target and the multiplication medium, could leave more degrees of freedom choosing the material of the spallation target and the windows separating it from the fuel assembly and coolant. This is surely an important advantage in this particular technologically difficult problem.

6 Conclusions

We have tried to elucidate the question if proton or deuteron induced reactions are more efficient in neutron production using the LAHET and MCNP code systems. The complete optimisation of the neutron production efficiency involves three major parameters of interest: a) the energy spectra of neutrons; b) the angular distributions of neutrons; c) the averaged neutron multiplicities. Each of these parameters might be considered as the function of a chosen projectile, its total incident energy and a chosen target material, what makes our initial task even more complicated.

We found that neutron production by deuterons is higher by a factor of 2.5-1.3 (depending on incident energy) for light target (converter) like beryllium if compared to proton induced reactions. In the case of intermediate targets like iron, deuterons are more favourable by a factor of 1.4. However, for heavy target materials like uranium, both projectiles are equally efficient within 10% at higher incident energies.

A combination of deuterons together with a light target (converter) material gives the hardest neutron spectrum. Moreover, for all targets deuterons give higher yield of more energetic neutrons as compared to proton induced reactions. The most isotropic angular distribution of neutrons is obtained in the p+U reaction, while the d+Be reaction resulted in the most forward peaked neutrons.

These findings provided useful characteristics for the choice of the target material (heavy/light or combination of both) and the incident particle (proton/deuteron) for a sub-critical hybrid system. Four simplified cases of the sub-critical fuel assembly were considered: protons or deuterons bombarding the U or Be spallation targets placed inside the fissionable fuel assembly. We found that that the direct bombardment of heavy metal primary target (U+U case) gives

5-10% higher neutron yield per incident particle for deuterons than for protons at the same total energy. In the case of deuterons, the combined light metal primary target (Be+U case) results in nearly the same neutron yield as bombarding a heavy metal directly. Now the heat is distributed over a much greater depth since more energetic neutrons are produced. Proton induced reactions result in much smaller neutron multiplicities in this case.

Last but not the least, we predicted that the optimum energy gain in a hybrid system may be reached at lower incident energies if deuterons are used instead of protons and light metal target is employed as a spallation target. This lower energy should result in higher beam intensities, lower costs of the system and facilitate radioprotection problems. These findings should be confirmed by new experimental data in the domain below 600MeV. The use of deuterons and a separation of the whole target system into two, nearly independent, units could allow much broader choice of the primary target materials from very light elements to very heavy ones, what may be extremely useful in the difficult interface between the accelerator and the reactor. The present studies showed, that all characteristics are dependent on details of composition and geometry of the target, the multiplying medium and the moderator. The present conclusions will hold, to our opinion, qualitatively for other configurations; however, one always must take into account the precise device for a realistic optimisation.

7 Acknowledgments

We wish to express our appreciation to Dr. R.E.Prael (Los Alamos National Laboratory) for providing us with the LAHET code system. We also thank the Radiation Shielding Information Center (Oak Ridge National Laboratory) for providing us with the MCNP code system through the NEA Data Bank. We are very grateful to Dr. S.Leray for sharing with us the information on so called "Status of the MTA Process" issued in February 1954 by Livermore Research Library.

References

- [1] L.C. Hebel *et al.*, Rev. Mod. Phys. **50** (1978) 1
- [2] C.D.Bowman *et al.*, Nucl. Instr. & Meth. **A 320** (1992) 336
- [3] C. Rubbia *et al.*, "Conceptual design of a fast neutron operated high power energy amplifier", preprint CERN/AT/95-44 (ET) (1995)

- [4] H. Nifenecker and M. Spiro, "Hybrid systems for waste incineration and/or energy production", Journées GEDEON, Cadarache (November 1997)
- [5] Concept for Advanced Exotic Beam Facility Based on ATLAS, Argonne National Laboratory (February 1995)
- [6] Journée de Reflexion, SPIRAL Phase 2, Rapport Interne, GANIL (September 1997)
- [7] Status of the MTA process, LRL-102, Livermore Research Laboratory (February 1954)
- [8] R.E. Prael and H. Lichtenstein, "User Guide to LCS: The LAHET Code System," Los Alamos National Laboratory Report LA-UR-89-3014 (September 1989)
- [9] H.W. Bertini, Phys. Rev. **131** (1963) 1801
- [10] A. Mignerey *et al.*, Nucl. Phys. **A 273** (1976) 125
- [11] J.J. Griffin, Phys. Rev. Lett. **17** (1966) 478
- [12] M. Blann, Phys. Rev. Lett. **21** (1968) 1357
- [13] M. Blann, Phys. Rev. Lett. **28** (1972) 757
- [14] H.W. Bertini, Phys. Rev. **188** (1969) 1711
- [15] Y. Yariv and Z. Fraenkel, Phys. Rev. **C 20** (1979) 2227
- [16] K. Chen *et al.*, Phys. Rev. **166** (1968) 949
- [17] M.R. Clover, R.M. DeVries, N.J. DiGiacomo and Y. Yariv, Phys. Rev. **C 26** (1982) 2138
- [18] J. Barish *et al.*, ORNL/TM-7882, Oak Ridge National Laboratory (July 1981)
- [19] F. Atchison, "Spallation and Fission in Heavy Metal Nuclei under Medium Energy Proton Bombardment" in "Targets for Neutron Beam Spallation Sources", Jül-Conf-34, Kernforschungsanlage Jülich GmbH (January 1980)

- [20] L. Dresner, ORNL/TM-196, Oak Ridge National Laboratory (April 1962)
- [21] D.J. Brenner, R.E. Prael, J.F. Discello and M. Zaider, "Improved Calculations of Energy Deposition from Fast Neutrons", in Proceedings Fourth Symposium on Neutron Dosimetry, EUR-7448, Munich-Neuherberg (1981)
- [22] R.E. Prael and M. Bozoian, LA-UR-88-3238, Los Alamos National Laboratory (September 1988)
- [23] Group X-6, "A General Monte Carlo Code for Neutron and Photon Transport", LA-7396-M, Los Alamos National Laboratory (April 1981)
- [24] More detailed information can be provided by one of the authors (D.R.) of this manuscript if requested by e-mail (ridikas@ganil.fr)
- [25] D. Ridikas and W. Mittag, GANIL preprint **P 97 19**, GANIL, Caen (May 1997)
- [26] J.P. Meulders, P. Leleux, P.C. Macq and C. Pirart, Phys. Med. Biol. **Vol. 20, No. 2** (1975) 235
- [27] B. Lott *et al.*, GANIL preprint **P 97 37**, GANIL, Caen (December 1997)
- [28] L. Pienkowski *et al.*, Phys. Lett. **B 336** (1994) 147
- [29] E. Martinez, These le Grade de Docteur de l'Universite de Caen, Caen (May 1997)
- [30] J. Cugnon, C. Volant and S. Vuillier, Nucl. Phys. **A 625** (1997) 729
- [31] C. Volant, private communication, CEA, Saclay (December 1997)
- [32] C.M. Van Atta, "A brief history of the MTA project", unpublished
- [33] S. Andriamonje *et al.*, Phys. Lett. **B 348** (1995) 697

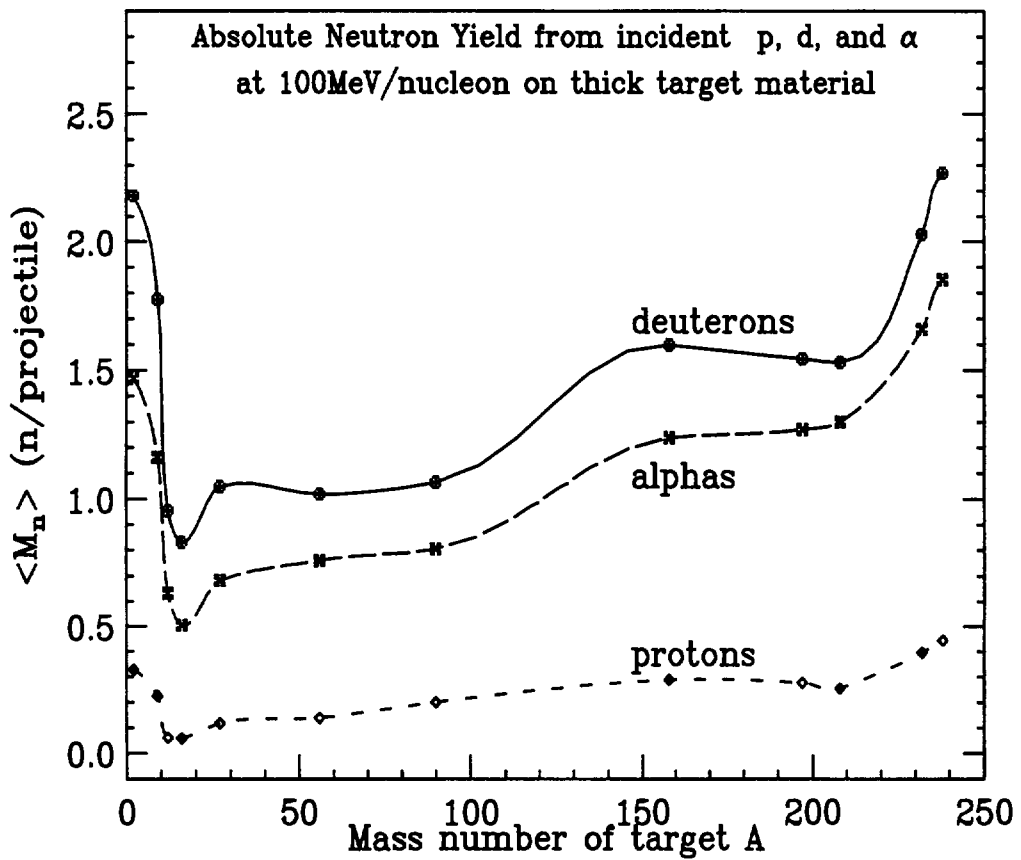


Figure 1: Calculated neutron multiplicities $\langle M_n \rangle$ as a function of a thick (5 ranges for deuterons) target material A for p , d and α particles at 100 MeV per nucleon.

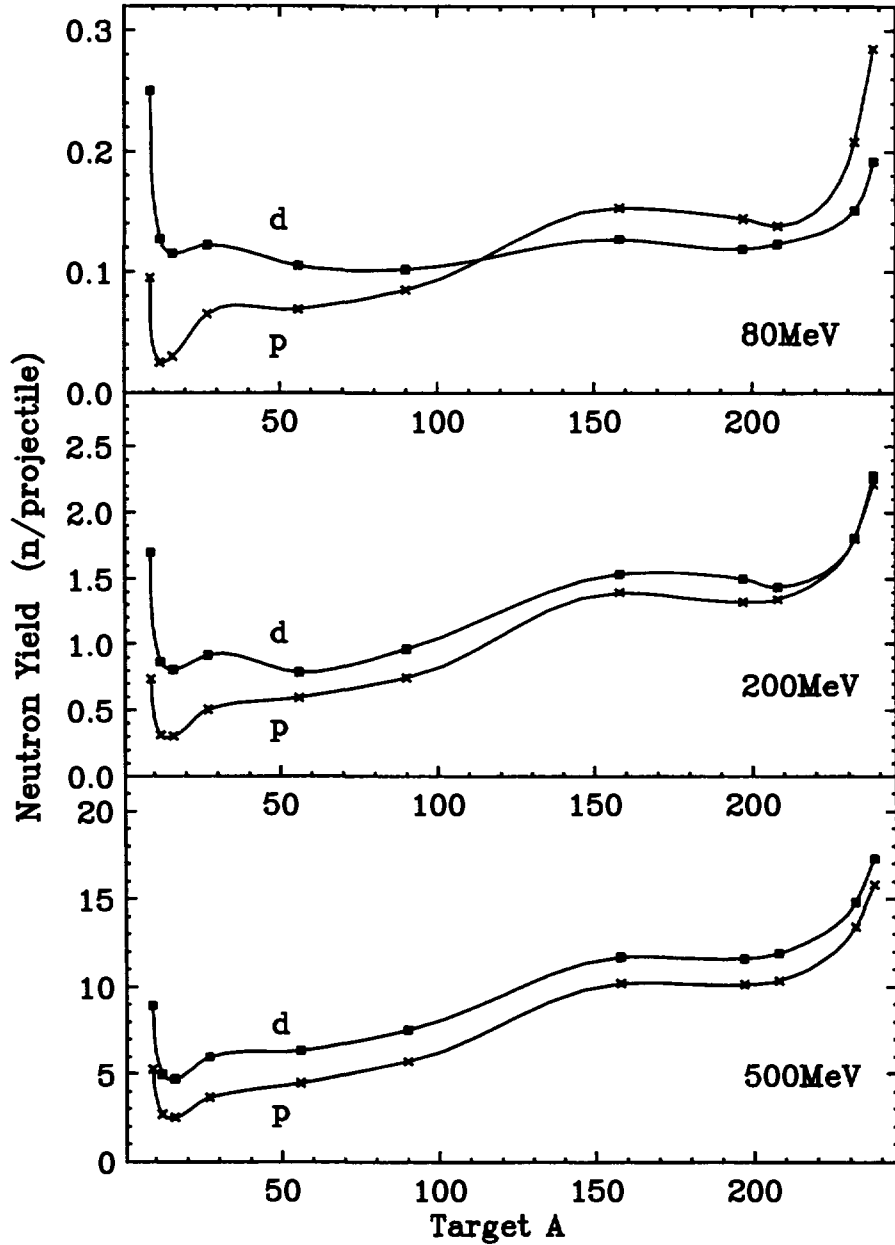


Figure 2: Estimate of neutron production by protons and deuterons with total incident energies of 80MeV, 200MeV and 500MeV. A thick target is a cylinder with equal length and diameter given by 2 ranges for protons depending on incident energy.

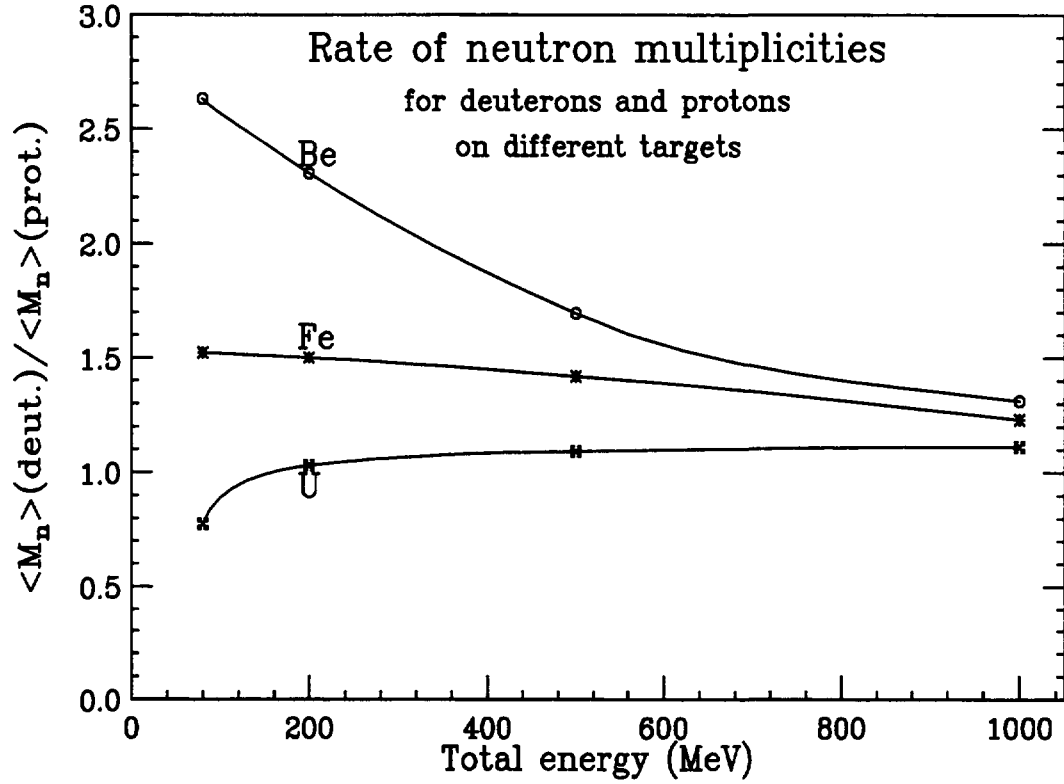


Figure 3: Calculated ratio of neutron multiplicities from deuteron induced reactions over proton induced reactions on different target materials as a function of the total incident energy of the projectiles. A thick target is a cylinder with equal length and diameter given by 2 ranges for protons depending on incident energy.

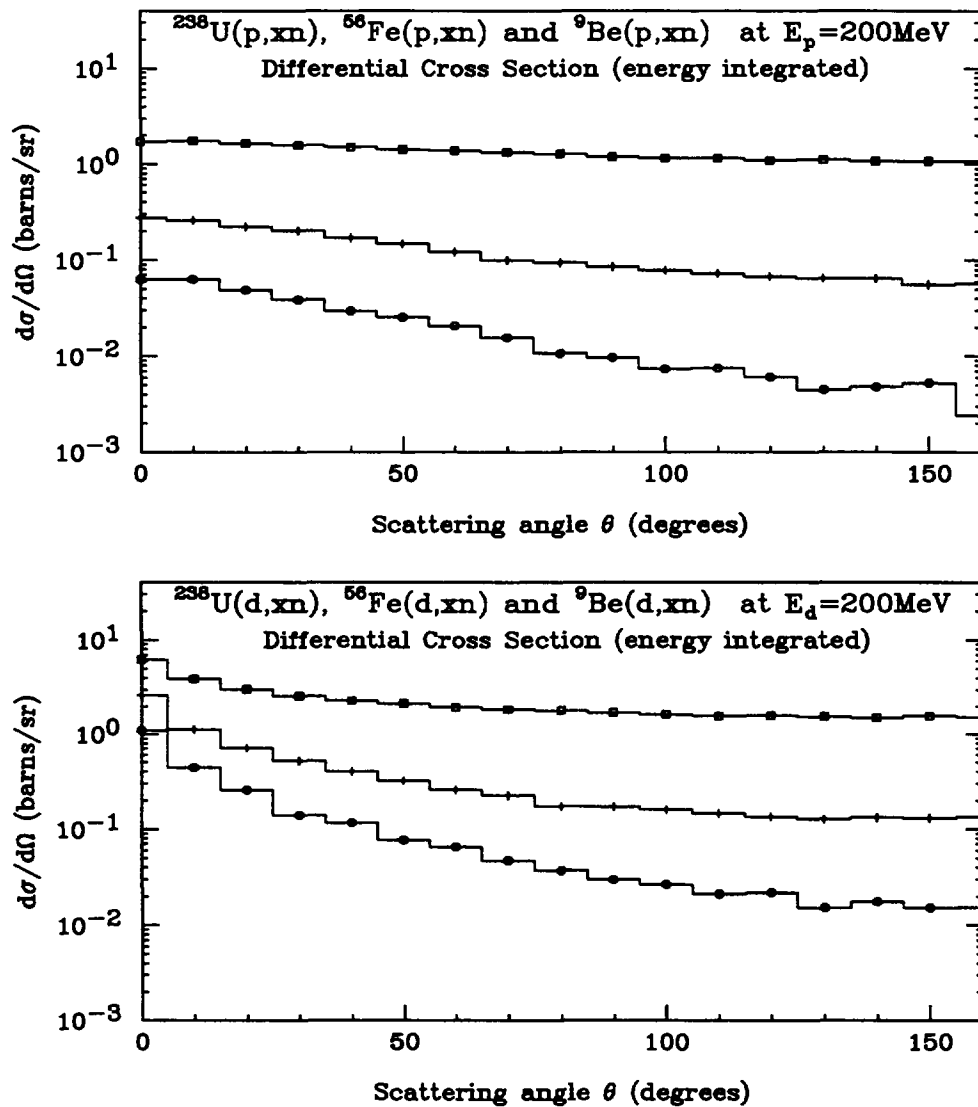


Figure 4: Calculated angular distributions of neutron production cross sections for incident protons (upper) and deuterons (lower) on three targets, i.e. U, Fe and Be from top-to-bottom respectively. Total incident energy is chosen to be 200MeV for both of the projectiles.

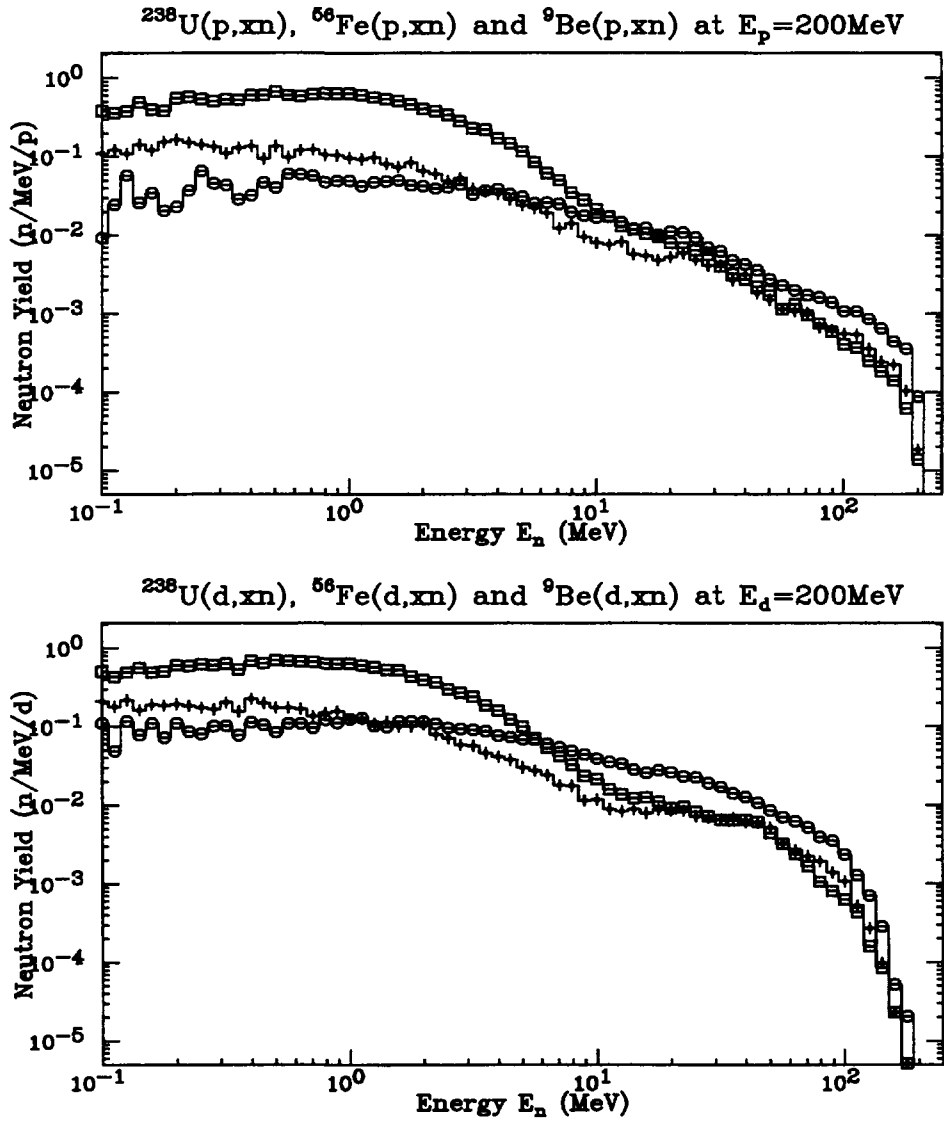


Figure 5: Predicted neutron energy distributions for incident protons (above) and deuterons (below) on three targets, i.e. U, Fe and Be from top-to-bottom respectively at the lowest neutron energies. Total incident energy is 200MeV for both of the projectiles. A thick target is a cylinder with equal length and diameter given by 2 ranges for protons.

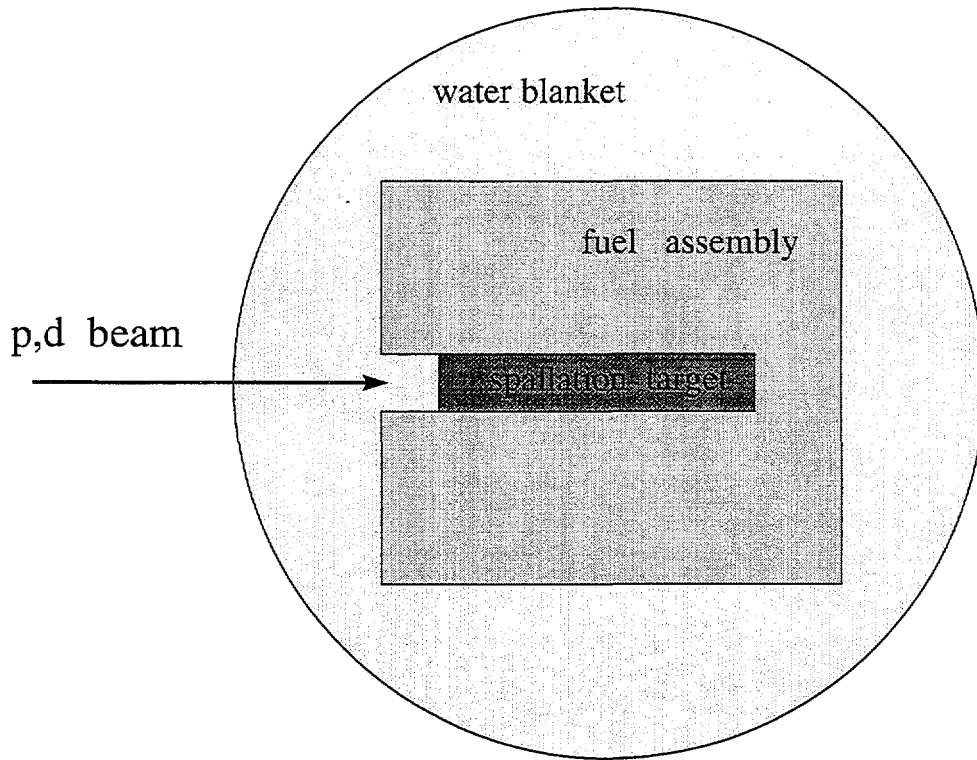


Figure 6: A simplified sub-critical target assembly for neutron multiplication and energy production with incident protons or deuterons (see Table 3 for detailed geometry and material parameters). The target units preserve a symmetry along the beam axis.

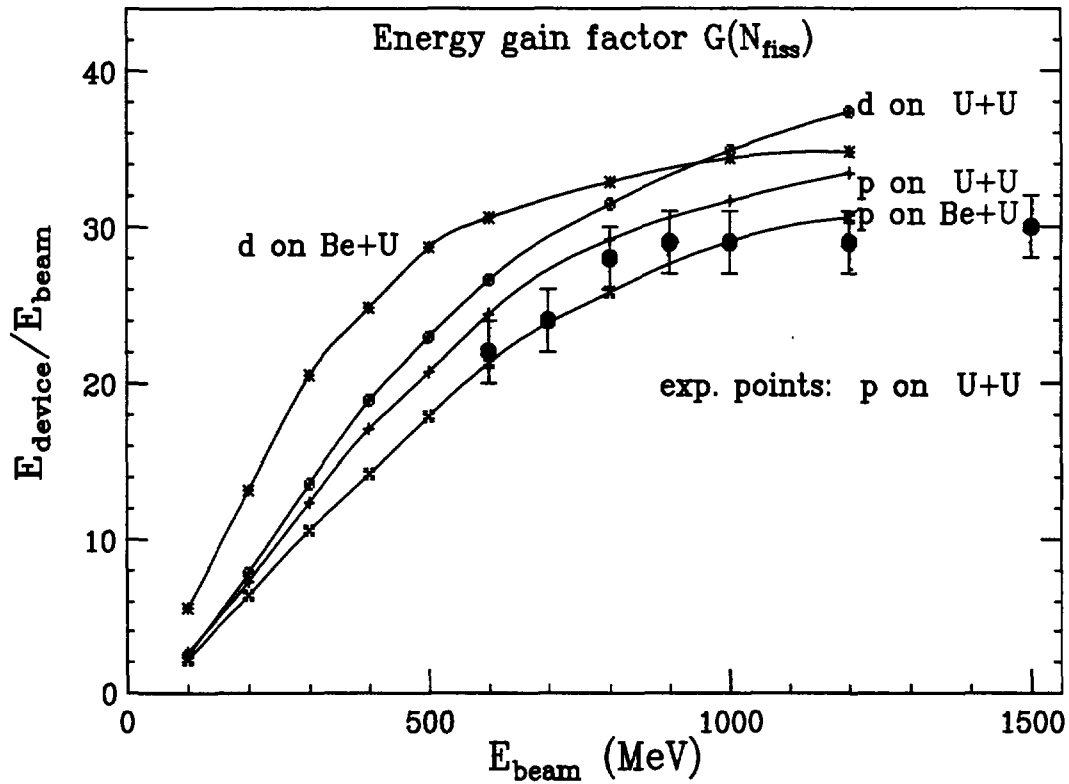


Figure 7: Calculated and measured [33] average energy gain, i.e. the ratio of the energy produced by fissions in the device to the energy delivered by the beam, for proton and deuteron induced reactions on different target assemblies as a function of beam kinetic energy (see Tables 4 and 5 and Fig. 6 for details).

E (MeV)	⁹ Be	⁵⁶ Fe	²³⁸ U
80	3.4	1.0	0.6
200	17.2	4.8	3.0
500	77.0	21.0	12.7
1000	215.0	60.0	35.0

Table 1: Stopping ranges for protons in (cm) as a function of incident energy and target material. The following equation is used for evaluation the ranges for deuterons: $R_d(E)=2R_p(\frac{1}{2}E)$, where E is the total energy of a projectile.

	⁹ Be		⁵⁶ Fe		²³⁸ U	
E_n (MeV)	p	d	p	d	p	d
≥ 0	0.737	1.700	0.594	0.898	2.216	2.283
≥ 5	0.525	1.233	0.282	0.475	0.490	0.585
≥ 10	0.420	0.980	0.216	0.388	0.276	0.399
≥ 25	0.243	0.575	0.129	0.263	0.131	0.233
≥ 50	0.131	0.250	0.062	0.110	0.054	0.082
≥ 100	0.051	0.031	0.021	0.012	0.015	0.009

Table 2: Predicted neutron multiplicities $\langle M_n \rangle$ per deuteron and proton respectively for different thick target materials and different energies of emitted neutrons. Total incident energy is chosen to be 200MeV for both of the projectiles. A thick target has a cylinder geometry with equal length and diameter given by 2 ranges for protons.

	Materials	Dimensions
spallation targets (cylinder)	${}^9\text{Be}$ or ${}^{238}\text{U}$	$r_c=3.5\text{cm}$; $l=R_p$ or $l=R_d$ $r_c=3.5\text{cm}$; $l=80.0\text{cm}$
fuel assembly (cylinder)	$0.373 \text{ U} + 0.627 \text{ H}_2\text{O}$, where $\text{U} = {}^{235}\text{U}(0.95\%) + {}^{238}\text{U}(99.05\%)$	$r_c=45.0\text{cm}$; $l=110.0\text{cm}$
water blanket (sphere)	H_2O	$r_s=75.0\text{cm}$

Table 3: Parameters of the sub-critical target assembly shown in Fig. 6. Here l is the length of a cylinder with its radius given by r_c ; r_s is the radius of a sphere, R_p and R_d correspond to the stopping ranges for protons and deuterons respectively (see Table 1 for the ranges at different incident energies). Note: $l=R_p$ (or $l=R_d$) applies only if R_p (or R_d) is smaller than 80cm; otherwise, $l=80\text{cm}$ is used in the case of ${}^9\text{Be}$. For ${}^{238}\text{U}$ spallation target with $l=80\text{cm}$ is considered.

E_{beam} (MeV)	$\langle M_n \rangle$		N_{fiss}		$G(\langle M_n \rangle)$		$G(N_{fiss})$	
	p	d	p	d	p	d	p	d
100	0.54	0.51	1.44	1.35	3.03	2.85	2.61	2.44
200	2.72	3.04	8.06	8.64	7.67	8.57	7.29	7.82
300	6.82	7.37	20.48	22.47	12.80	13.84	12.36	13.56
400	11.91	12.69	37.75	40.04	16.79	17.89	17.08	18.89
500	17.72	19.85	57.19	63.39	19.95	22.34	20.70	22.94
600	24.38	26.92	80.88	88.25	22.87	25.24	24.40	26.62
800	37.95	42.09	129.03	139.06	26.70	29.61	29.20	31.46
1000	51.01	56.78	174.85	192.58	28.76	32.02	31.65	34.86
1200	63.06	72.28	221.58	247.79	29.54	33.86	33.42	37.35

Table 4: Predicted neutron multiplicities $\langle M_n \rangle$, number of fissions N_{fiss} and G-factors per incident deuteron (d) or proton (p) respectively as a function of the total available beam energy E_{beam} for a sub-critical device with the uranium spallation target inside the fuel assembly (see Fig. 6 and Table 3 for details).

E_{beam} (MeV)	$\langle M_n \rangle$		N_{fiss}		$G(\langle M_n \rangle)$		$G(N_{fiss})$	
	p	d	p	d	p	d	p	d
100	0.36	0.87	1.18	3.07	2.13	5.22	2.14	5.56
200	1.91	4.03	7.08	14.53	5.73	12.09	6.41	13.15
300	4.49	8.87	17.51	33.99	8.98	17.74	10.56	20.50
400	7.98	14.14	31.36	54.89	11.98	21.22	14.19	24.82
500	12.26	20.67	47.73	79.31	14.72	24.84	17.28	28.71
600	18.11	26.20	70.60	101.43	18.12	26.20	21.30	30.60
800	29.06	37.77	114.07	145.33	21.79	28.32	25.81	32.88
1000	40.68	49.31	160.58	189.96	24.37	29.54	29.07	34.38
1200	50.97	60.09	202.87	230.74	25.49	30.05	30.60	34.80

Table 5: Predicted neutron multiplicities $\langle M_n \rangle$, number of fissions N_{fiss} and G-factors per incident deuteron (d) or proton (p) respectively as a function of the total available beam energy E_{beam} for a sub-critical device with the beryllium spallation target inside the fuel assembly (see Fig. 6 and Table 3 for details).